



HAL
open science

Fluid selection for a low-temperature solar organic Rankine cycle

Tchanche Fankam Bertrand, George Papadakis, Gregory Lambrinos, Antonios Frangoudakis

► **To cite this version:**

Tchanche Fankam Bertrand, George Papadakis, Gregory Lambrinos, Antonios Frangoudakis. Fluid selection for a low-temperature solar organic Rankine cycle. *Applied Thermal Engineering*, 2009, 29 (11-12), pp.2468. 10.1016/j.applthermaleng.2008.12.025 . hal-00528081

HAL Id: hal-00528081

<https://hal.science/hal-00528081>

Submitted on 21 Oct 2010

HAL is a multi-disciplinary open access archive for the deposit and dissemination of scientific research documents, whether they are published or not. The documents may come from teaching and research institutions in France or abroad, or from public or private research centers.

L'archive ouverte pluridisciplinaire **HAL**, est destinée au dépôt et à la diffusion de documents scientifiques de niveau recherche, publiés ou non, émanant des établissements d'enseignement et de recherche français ou étrangers, des laboratoires publics ou privés.

Accepted Manuscript

Fluid selection for a low-temperature solar organic Rankine cycle

Tchanché Fankam Bertrand, George Papadakis, Gregory Lambrinos, Antonios Frangoudakis

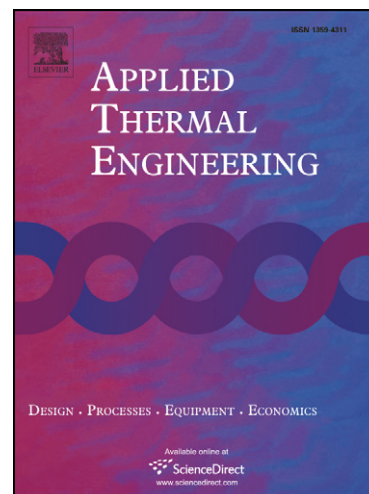
PII: S1359-4311(08)00490-0
DOI: [10.1016/j.applthermaleng.2008.12.025](https://doi.org/10.1016/j.applthermaleng.2008.12.025)
Reference: ATE 2695

To appear in: *Applied Thermal Engineering*

Received Date: 4 February 2008
Revised Date: 5 December 2008
Accepted Date: 16 December 2008

Please cite this article as: T.F. Bertrand, G. Papadakis, G. Lambrinos, A. Frangoudakis, Fluid selection for a low-temperature solar organic Rankine cycle, *Applied Thermal Engineering* (2008), doi: [10.1016/j.applthermaleng.2008.12.025](https://doi.org/10.1016/j.applthermaleng.2008.12.025)

This is a PDF file of an unedited manuscript that has been accepted for publication. As a service to our customers we are providing this early version of the manuscript. The manuscript will undergo copyediting, typesetting, and review of the resulting proof before it is published in its final form. Please note that during the production process errors may be discovered which could affect the content, and all legal disclaimers that apply to the journal pertain.



Fluid selection for a low-temperature solar organic Rankine cycle

Tchanche Fankam Bertrand*, George Papadakis, Gregory Lambrinos and
Antonios Frangoudakis

Department of Natural Resources and Agricultural Engineering,
Agricultural University of Athens, 75 Iera Odos Street 11855 Athens-Greece
Tel.: +30 (210) 529 4046; Fax: +30 (210) 529 4032

* Corresponding author, e-mail address: tfb@aua.gr, tfb_tchanchef@yahoo.fr

Abstract

Theoretical performances as well as thermodynamic and environmental properties of few fluids have been comparatively assessed for use in low-temperature solar organic Rankine cycle systems. Efficiencies, volume flow rate, mass flow rate, pressure ratio, toxicity, flammability, ODP and GWP were used for comparison. Of 20 fluids investigated, R134a appears as the most suitable for small scale solar applications. R152a, R600a, R600 and R290 offer attractive performances but need safety precautions, owing to their flammability.

Keywords: Small Scale Solar Applications, Working Fluids, Organic Rankine Cycle

Nomenclature

h	Enthalpy	(kJ/kg)	p	Pump
\dot{I}	Irreversibility	(kW)	pp	Pinch point
\dot{m}	Mass flow rate	(kg/s)	s	Isentropic
P	pressure	(MPa)	t	Turbine
PR	Pressure ratio	(-)	th	Thermal
\dot{Q}	Heat rate	(kW)	tot	Total
s	Entropy	(kJ/kg.K)	uhx	Upper heat exchangers
T	Temperature	(°C)	wf	Working fluid
\dot{V}	Volume flow rate	(m ³ /h)		
VFR	Volume flow ratio	(-)		
\dot{W}	Work	(kW)		<i>Acronyms</i>
x	Quality	(-)	GWP	Global warming potential
			ODP	Ozone depletion potential
			ORC	Organic Rankine Cycle
	<i>Greek letters</i>			
ΔT	Temperature difference	(°C, K)		
Δh	Enthalpy difference	(kJ/kg)		
φ	Enthalpy ratio	(%)		
η	Efficiency	(%)		
v	Specific volume	(m ³ /kg)		
	<i>Subscript-superscript</i>			
0	Reference state			
$0,htf$	Preheater exit (hot side)			
$1-5$	States in the cycle			
amb	Ambient			
bp	Boiling point			
c	Condenser			
$crit$	Critical			
fg	Phase change			
i	Inlet			
II	Second law			
H	Heat source			
ht	Heat source-turbine			
htf	Heat transfer fluid			
L	Cold source			
m	Mechanical			
max	Maximum			
min	Minimum			

1. Introduction

Almost 2 billion people worldwide do not have access to electricity. Most of these electricity-deprived live in sub-Saharan Africa and south Asia. Usually, these populations live in remote areas far from the centralized electricity grid with very low income and extending the electricity grid is not seen as economically feasible for electricity companies which prefer to concentrate their activities in urban areas. On the other hand, existing conventional power plants use fossil fuels or radioactive materials as inputs, and are integrated in centralized systems. Derived consequences are power losses in transportation lines due to the remoteness of the electricity infrastructure from the consumers and environmental pollution. Pollutants released in the atmosphere are responsible of the ozone depletion, global warming, acid rains and contamination of lands and seas. In this context, using renewable energies like solar energy, wind energy, biomass and geothermal heat as well as waste heat for electricity production becomes important.

In recent years, organic rankine cycle has become a field of intense research and appears as a promising technology for conversion of heat into useful work or electricity. The heat source can be of various origins: solar radiation, biomass combustion, ground heat source or waste heat from factories. Unlike in the steam power cycle, where vapor steam is the working fluid, organic Rankine cycles (ORC) employ refrigerants or hydrocarbons. Quoilin et al [1], Nguyen et al. [2], Saitoh et al. [3], Kane et al. [4] and Yagoub et al. [5] proposed and studied different micro-ORCs designed for electricity generation. Fenton et al [6] reported an irrigation system based on an ORC conversion module using R113 as working fluid. Prigmore and Barber [7] and Kaushik et al. [8] investigated cooling systems coupled with Rankine engines. Manolakos et al. [9-10], Schuster et al. [11] and Bruno et al. [12] are some researchers who proposed the use of ORC technology for seawater desalination. Wei et al. [13], Nowak et al. [14], Hung

[15] and Liu et al. [16] studied and analyzed the performance of ORCs for waste heat recovery. In view of increasing the system efficiency, Kauschick et al. [8], Mago et al. [17] and Tchanche et al. [18] assessed modified ORC configurations.

The economics of a Rankine system is strictly linked to the thermodynamic properties of the working fluid [19]. A bad choice could lead to a low efficient and expensive plant. Criteria that should fulfill a fluid for its suitability in ORCs were reported by some researchers and are summarized in a previous work [20]. Properties of a good fluid are: low specific volumes, high efficiency, moderate pressures in the heat exchangers, low cost, low toxicity, low ODP and low GWP among others. Maizza and Maizza [21], Badr et al. [22], Saleh et al. [23], Hettiarachchi et al. [24], Drescher and Brüggemann [25] and Yamamoto et al. [26] are some of the researchers who analyzed the characteristics of different working fluids in view of their selection in an ORC application. The International protocols [27] pushed researchers to investigate new environmentally friendly fluids which could serve as substitutes. Contributing in this direction, performance of carbone dioxide, synthetic and refrigerant mixtures were evaluated by Yamaguchi et al. [28], Angelino and Colonna di Paliano [29] and Borsukiewicz-Gozdur and Nowak [30] in different types of cycles.

The present work deals with the selection of most suitable fluids for a low-temperature solar organic Rankine cycle. Hot water serving as heat source at maximum temperature of 90 °C is produced by conversion of solar radiation into heat by solar collectors. A schematic of the system is shown in Fig. 1. Characteristics of 20 potential working fluids are evaluated and compared for a 2 kW micro-power system.

2. System modeling

The present ORC system consists of heat exchangers (pre-heater, boiler/evaporator), a micro-turbine/expander, a condenser and a pump. The micro-turbine considered here is similar to the scroll expander investigated by Manolakos et al. [10], Quoilin et al. [1] and Lemort [31]. The pump supplies the working fluid to the heat exchangers (preheater, evaporator) where it is heated and vaporized by the hot water from the collector array. The generated high pressure vapor flows into the expander and its enthalpy is converted into work. The low pressure vapor exits the expander and is led to the condenser where it is liquefied by air. The liquid available at the condenser outlet is pumped back to the upper heat exchangers and a new cycle begins. All the above described processes are shown in a T-s diagram in Fig. 2.

Using First and Second Laws of thermodynamics [32], the performance of the ORC will be evaluated under diverse working conditions for different organic working fluids. For simplicity, the internal irreversibility and, accordingly the pressure drops in the components other than the turbine, such as the preheater, evaporator, condenser and pipes, are ignored. For each individual component, first and second laws of thermodynamics are applied to find the work output or input, the heat added or rejected, and the system irreversibility. The equations obtained are summarized below.

Expander $\dot{W}_t = \dot{m}_{wf} (h_1 - h_{2s}) \eta_{st} \eta_{mt} = \dot{m}_{wf} (h_1 - h_2) \eta_{mt}$ (1)

$$\dot{I}_t = T_0 \dot{m}_{wf} (s_2 - s_1) \quad (2)$$

Condenser $\dot{Q}_c = \dot{m}_{wf} (h_2 - h_3)$ (3)

$$\dot{I}_c = T_0 \dot{m}_{wf} \left[(s_3 - s_2) - \frac{h_3 - h_2}{T_L} \right] \quad (4)$$

Upper Heat Exchangers $\dot{Q}_{uhx} = \dot{m}_{wf} (h_1 - h_4)$ (5)

$$\dot{I}_{uhx} = T_0 \dot{m}_{wf} \left[(s_1 - s_4) - \frac{h_1 - h_4}{T_H} \right] \quad (6)$$

Pump $\dot{W}_p = \dot{m}_{wf} v_3 (P_4 - P_3) / \eta_p$ (7)

$$\dot{I}_p = T_0 \dot{m}_{wf} (s_4 - s_3) \quad (8)$$

First Law Efficiency $\eta_{th} = (\dot{W}_t - \dot{W}_p) / \dot{Q}_{uhx}$ (9)

Second Law Efficiency $\eta_{II} = \eta_{th} / (1 - T_L / T_H)$ (10)

System Total Irreversibility $\dot{I}_{tot} = \sum_j \dot{I}_j = T_0 \dot{m}_{wf} \left[-\frac{h_1 - h_4}{T_H} - \frac{h_3 - h_2}{T_L} \right]$ (11)

Input Enthalpy Ratio $\varphi = \frac{h_1 - h_5}{h_1 - h_4} = \frac{\Delta h_{fg}}{\Delta h_{tot}}$ (12)

3. Results and discussion

The operating conditions of the ORC are given in Tale 1 along with the characteristics of the expander and the pump. Hot water at 90 °C is provided by solar collectors. The condenser is cooled by ambient air. The system is assumed to be located in a hot area where the average monthly ambient temperature is around 28 °C. Fig. 3 shows the yearly variations of the ambient temperature for such locations [33].

As result of a first screening, 20 fluids presented in Table 2 emerged as potential candidates. Only one criterion was considered at this first step: critical temperature above 75 °C. In this study, we consider a subcritical cycle where the vapor at the turbine inlet is saturated. The superheat was not found of interest as the incorporation of a superheater could bring additional cost. The thermodynamic properties of fluids and system performance are evaluated with a simulation tool EES (Engineering Equation Solver) [34]. The results are displayed in Table 3 for a designed 2 kW power output.

3.1 Cycle pressure

According to Badr et al. [22] and Maizza and Maizza [21], good pressure values are in the range 0.1-2.5 MPa and a pressure ratio (PR) of about 3.5 is reasonable. From Table 3, the following observations can be made concerning the pressure in the condenser and the upper heat exchangers. R113, cyclohexane, methanol, water and ethanol present low condenser pressures. R407C, R32 and R717 have higher pressures above 3 MPa in the evaporator. Methanol, water, ethanol, cyclohexane and R113 have higher pressure ratio. Ethanol and water have low evaporating pressure. Isentropic fluids present pressure values that fall in the range prescribed by the above cited authors, and therefore are good fluids from a pressure point of view. Other fluids with good condensing and evaporating pressures are: RC318, R600a, R600, R114, R601, R500 and R152a.

3.2 Turbine outlet volume flow rate

Turbine outlet volume flow rate determines its size and the system cost. Results of calculations in Table 3 let see that n-Pentane, R113, cyclohexane, water, ethanol, methanol, R123 and R141b exhibit high volume flow rates. Fluids with low volume flow rate are preferable for economic reasons. Among these are: R32, Ammonia, R407C, R290, R500, R134a and R152a. From Fig. 4 It is seen that in general, the volume flow rate decreases with an increment of temperature. A prediction for fluids not suitable in the range of temperature considered here to be at higher temperature can be raised.

3.3 Cycle efficiency

The system thermal efficiency ranges from 2.61% for R32 to 4.89% for water. Figs. 5-6 show the effects of the variation of the turbine inlet pressure. The temperature difference ΔT_{ht} is maintained constant and the vapor at the expander inlet saturated. The system thermal efficiency increases with a raise of the turbine inlet pressure. For high boiling point fluids water and ethanol are more efficient compared to n-Pentane and R123 (Fig. 6). In Table 3, the second law efficiency varies from 15.3% (R32) to 28.7% (water). Effects of the turbine inlet pressure on the system second law efficiency can be seen on Figs. 7-8. For low boiling point fluids, second law efficiency shows a maximum (Fig. 7) which suggests the existence of an optimal operating condition. System second law efficiency for the second group increases in a short range 0-1.0 MPa and decreases slightly for higher pressures (Fig. 8).

3.4 Irreversibility

From Table 3, system total irreversibility varies in the range 3.79-5.15 kW. Water and R407C yield the lowest and highest irreversibility rates, respectively. Fig. 9 shows the irreversibility distribution for different components and for different fluids. It can be seen that the upper heat exchangers (preheater, evaporator) are the components that have the biggest contribution to the overall irreversibility followed by the turbine. Both components account for about 78% of the system total irreversibility.

The system irreversibility was analyzed based on the changes of some parameters. In order to study the effects of the heat source temperature on the system irreversibility, the temperature difference between the heat source and the turbine inlet was maintained constant ($\Delta T_{ht}=15\text{ }^{\circ}\text{C}$). While varying the turbine inlet temperature and keeping the working fluid state along the vapor saturation curve, Figs. 10-11 show the effects of the heat source temperature on the system irreversibility. In Fig. 10, the system total irreversibility decreases faster for low boiling points fluids as the operation pressure at the turbine inlet increases and reaches a limit of 4 kW. The lowest irreversibility rate is obtained for RC318. In Fig. 11, the system total irreversibility increases as the pressure at the turbine inlet increases. For this category, the system irreversibility is lower compared to fluids with low boiling points temperature. Water yields the lowest irreversibility rate followed by methanol and ethanol.

In the second part of the analysis, the temperature of the heat source was kept constant. As shown in Figs. 12-13, the system total irreversibility decreases as the turbine inlet pressure increases. As conclusion, small temperature difference between the fluid streams improves the system's performance.

3.5 Mass flow rate

From Table 3, water, ethanol and methanol yield lowest maximum pressures and highest enthalpy heat of evaporation (Δh_{fg}). This is an advantage for these fluids which will require lower mass flow rates, and hence lower heat input. Ammonia, has a higher evaporating pressure, but yields a low mass flow rate and high heat of vaporization. From Fig. 14, it can be seen that the system mass flow rate decreases when the turbine inlet temperature increases. For economical reasons, fluids with low mass flow rates like ammonia, ethanol and methanol are interesting especially for large capacity systems.

3.6 Analysis of the heat input

System heat input is of great importance in a solar ORC. It determines the size of the collector array and constitutes major part of system cost. Therefore, solar applications will be more competitive with fluids for which the amount of heat required is small. From Table 3, the heat required for a 2 kW power output falls in the range 40-47 kW. Fluids with high Δh_{fg} require low heat rates; these are: water, ethanol, methanol and ammonia. From Fig. 15, high temperature saturated vapors reduce the amount of heat input. This let us think that when designing a solar ORC, depending on the application, one could choose between system with large collector area-low temperature and a system with small collector area-high operating temperature.

3.7 Influence of the ambient temperature

Figs. 16 and 17 show the effects of the ambient temperature on the performance of the system. The fluid used for the analysis is the R134a. From Fig. 16, it is obvious that the ambient temperature greatly affects the condenser. As the ambient temperature gets close to the condenser temperature, the condenser irreversibility and hence the system

total irreversibility is reduced. Seeking for better performance, we suggest reasonable temperature difference between the condenser temperature and the ambient temperature be taken in the range 5-15 °C.

3.8 Study of the heat transfer in the heat exchangers

The heat exchange process between the heat transfer fluid and the working fluid is studied using the energy balance in the upper heat exchangers. It can be expressed as:

$$\dot{m}_{\text{htf}} (h_{\text{H}} - h_{\text{pp,htf}}) = \dot{m}_{\text{wf}} (h_1 - h_{\text{pp,wf}}) \quad (13)$$

$$\dot{m}_{\text{htf}} (h_{\text{pp,htf}} - h_{\text{o,htf}}) = \dot{m}_{\text{wf}} (h_{\text{pp,wf}} - h_4) \quad (14)$$

Where \dot{m}_{htf} and \dot{m}_{wf} are the mass flow rates of heat transfer fluid and working fluid, respectively. $h_{\text{pp,htf}}$ and $h_{\text{pp,wf}}$ are the enthalpies of the heat transfer fluid and the working fluid at the pinch point, respectively. $h_{\text{o,htf}}$ is the enthalpy of the heat transfer fluid after leaving the upper heat exchangers. The set pinch-point temperature difference is $\Delta T_{\text{pp}} = 6$ °C. Figs. 18, 19 and 20 show the temperature profiles in the upper heat exchangers for three working fluids: R134a, methanol and R407C. The temperature profiles depend on the properties of the fluids: latent heat of vaporization, the shape of the saturation curve, the thermal conductivity among others. From Figs. 18-20, the heat amounts transferred to the cycle through the preheater and evaporator depend upon the fluid. Therefore, the pinch point analysis should be considered when designing the system for an efficient heat transfer in the preheater and evaporator. From Figs. 18-19, unlike methanol which requires a small preheater and a large evaporator R134a will require larger preheater and smaller evaporator. Using methanol, most of the heat will be transferred during the phase change; this is due to the fact that at 75 °C, methanol possesses high latent heat of vaporization. In case of a zeotropic fluid

(R407C), the temperature varies during the phase change. Where we do not master the consequence of such behavior, we will not address it here.

In Table 4 are displayed the following parameters: the temperature of the heat transfer fluid leaving the preheater, pinch points for cold and hot fluids, the mass flow rates and the heat input for five working fluids. Ammonia and methanol have the lowest heat input rates and the lowest working fluid mass flow rates compared with other fluids. The heat input is an important parameter as it determines the size of the solar collector array and the volume of the heat store and hence, the cost of the system. Where we cannot conclude on the heat transfer fluid mass flow rate, we mention that for an efficient plant, low flow rates (10-15 l/m²h) are preferable in the collector loop. Based on the analysis done in this section, from an economic as from a heat transfer point of view, methanol and ammonia are good fluids.

3.9 Environmental considerations

Some substances, mainly refrigerants, deplete the ozone layer or/and contribute to the global warming. Because of their negative effects, there is a necessity to choose those with less harmful effects on the environment. R12, R113, R114 and R500 cannot be selected owing to their high ODP and high GWP. RC318 has a GWP of about 10250 and is excluded from the selection. Unfortunately, there is a lack of environmental data concerning some substances and this justifies the absence of some fluids in this analysis. There are few substances with low ODP or/and low GWP and these fluids used at present, will be phased-out in a near future. Among these are: R141b, R123, R407, R134a, R407C and R32. Water, ammonia, and alkanes families are environmentally friendly substances.

3.10 Safety considerations

Safety criteria cannot be omitted. ASHRAE 34 provides a safety classification for fluids. Alkanes non toxic but flammable are class A3. They require safety devices. R152a is classified A2 (lower flammability and non-toxic). R123 is B1 (non-flammable but toxic). Ammonia classified B2 (toxic and has lower flammability limit) could be used in an open space with lesser precaution compared with alkanes. R134a is of class A1 (non-flammable and non-toxic), i.e. safer compared to other refrigerants and therefore is the preferred fluid.

3.11 Over-all analysis

From the analyses carried out in the previous section (3.1-3.10), none of the fluids yields all the desirable properties. All the above mentioned parameters are important for ORC design. It is difficult to find an ideal working fluid which exhibits high efficiencies, low turbine outlet volume flow rate, reasonable pressures, low ODP, low GWP and is non-flammable, non-toxic and non-corrosive. In Table 5, a certain number of properties were regrouped. For a value of the parameter favoring the fluid, we put the sign + (plus), - (minus) in the opposite case and +/- when the drawback can be overcome or neglected. The following fluids are not selected:

- RC318 (high GWP)
- Cyclohexane (high volume flow rate, high pressure ratio)
- R407C (high evaporator pressure, low efficiency)
- R32 (high evaporator pressure, low efficiency, high moisture after expansion)
- Ethanol, water, methanol (non convenient pressure values, high turbine outlet volume flow rates)
- R12, R113, R114 and R500 (high GWP, high ODP)
- R141b (high turbine outlet volume flow rate, high ODP)

Finally, R134a followed by R152a, R290, R600 and R600a emerge as most suitable fluids for low-temperature applications with heat source temperature below 90 °C.

4. Conclusions

Thermodynamic characteristics and performances of different fluids were analyzed for selection as working fluids in a low temperature solar organic Rankine cycle. Several criteria were used for comparison: pressures, mass and volume flow rates, efficiencies, cycle heat input, safety and environmental data. Fluids favored by the pressure values are: isentropic fluids, butanes, N-pentane and refrigerants R152a, RC318 and R500. Low volume flow rates are observed for R32, R134a, R290, R500 and ammonia. High latent heat of vaporization presented by water, methanol, ethanol and ammonia has as consequences low mass flow rate and small heat input, which are advantages over the rest of fluids. From an efficiency point of view, fluids with high boiling point like ammonia, methanol, ethanol and water are very efficient but the presence of droplets during the expansion process is a drawback. Following the International regulations (Kyoto and Montreal Protocols), R12, R500, RC318, R114 and R113 are harmful for the environment. Concluding, R134a followed by R152a, R600, R600a and R290 are most suitable fluids for low-temperature applications driven by heat source temperature below 90 °C.

References

[1] S. Quoilin, M. Orosz and V. Lemort, Modeling and Experimental investigation of an organic rankine cycle using scroll expander for small solar applications, Proc. Eurosun Conference, Lisbon-Portugal, 7-10 Oct. 2008.

[2] V.M. Nguyen, P.S. Doherty, S.B. Riffat, Development of a prototype low-temperature Rankine cycle electricity generation system, Applied Thermal Engineering 21(2001) 169-181.

[3] T. Saitoh, N. Yamada, S. Wakashima, Solar rankine cycle system using scroll expander, Journal of Energy and Engineering, 2 (2007) 708-718.

[4] M. Kane, D. Larrain, D. Favrat, Y. Allani, Small hybrid solar power system, Energy 28 (2003) 1427-1443.

[5] W. Yagoub, P. Doherty, S.B. Riffat, Solar energy-gas driven micro-CHP system for an office, Applied thermal Engineering 26 (2006) 1604-1610.

[6] D.L. Fenton, G.H. Abernathy, G.A. Krivokapich, J.V. Otts, Operation and evaluation of the Willard solar thermal power irrigation system, Solar Energy 32 (1984) 735-751.

[7] D. Prigmore and R. Barber, Cooling with the sun's heat: Design considerations and test data for a Rankine cycle prototype, Solar Energy 17 (1975) 185-192.

- [8] S.C. Kaushik, A. Dubey, M. Singh, Steam rankine cycle cooling system: analysis and possible refinements, *energy conversion management*, 35 (1994) 871-886.
- [9] D. Manolakos, G. Papadakis, Essam Sh. Mohamed, S. Kyritsis, K. Bouzianas, Design of an autonomous low-temperature solar Rankine cycle system for reverse osmosis desalination, *Desalination* 183 (2005) 73-80.
- [10] D. Manolakos, G. Papadakis, S. Kyritsis, K. Bouzianas, Experimental evaluation of an autonomous low-temperature solar Rankine cycle system for reverse osmosis desalination, *Desalination* 203 (2007) 366-374.
- [11] A Schuster, J. Karl, S. Karellas, Simulation of an innovative stand-alone solar desalination system using an organic rankine cycle, *International Journal of Thermodynamics* 10 (2007) 155-163.
- [12] J. C. Bruno, J. Lopez-Villada, E. Letelier, S. Romera, A. Corona, Modelling and optimization of solar organic Rankine cycle engines for reverse osmosis desalination, *Applied Thermal Engineering* 28 (2008) 2212-2226
- [13] Donghong Wei, Xuesheng Lu, Zhen Lu, Jianming Gu, Performance analysis and optimization of organic Rankine cycle (ORC) for waste heat recovery, *Energy Conversion and Management* 4 (2007) 1113-1119.
- [14] W. Nowak, A. Borsukiewicz-Gozdur, A.A. Stachel, using the low-temperature Clausius-Rankine cycle to cool technical equipment, *Applied Energy* 85 (2008) 582-588.

- [15] T.C. Hung, Waste heat recovery of organic Rankine cycle using dry fluids, *Energy Conversion and Management* 42 (2001) 539-553.
- [16] B.T. Liu, K.H. Chien, C.C. Wang, Effect of working fluids on organic Rankine cycle for waste heat recovery, *Energy* 29 (2004) 1207-1217.
- [17] P.J. Mago, L.M. Chamra, K. Srinivasan, C. Somayaji, An examination of regenerative organic rankine cycles using dry fluids, *Applied Thermal Engineering* 28 (2008) 998-1007.
- [18] B. Fankam Tchanche, G. Papadakis, G. Lambrinos, A. Frangoudakis (2008): Effects of regeneration on low-temperature solar organic Rankine cycles, *Proc. Eurosun Conference, Lisbon-Portugal, 7-10 Oct. 2008*.
- [19] W. C. Andersen and T. J. Bruno, Rapid screening of fluids for chemical stability in organic rankine cycle applications, *Ind. Eng. Chem.* 44 (2005) 5560-5566.
- [20] B. F. Tchanche, G. Papadakis, G. Lambrinos, A. Frangoudakis (2008): Criteria for working fluids selection in low-temperature solar organic Rankine cycles, *Proc. Eurosun Conference, Lisbon-Portugal, 7-10 Oct. 2008*.
- [21] V. Maizza, A. Maizza, Working fluids in non-steady flows for waste energy recovery systems, *Applied Thermal Energy* 16 (7) (1996) 579-590.

- [22] O. Badr, S.D. Probert and P.W. O'Callaghan, Selecting a working fluid for a Rankine-Cycle Engine, *Applied Energy* 21 (1985) 1-42.
- [23] B. Saleh, G. Koglbauer, M. Wendland, J. Fischer, Working fluids for low-temperature organic Rankine cycles, *Energy* 32 (2007) 1210-1221.
- [24] H.D.M. Hettiarachchi, M. Golubovic, W.M. Worek, Yasuyuki Ikegami, Optimum design criteria for an organic Rankine cycle using low-temperature geothermal heat sources, *Energy* 32 (2007) 1698-1706.
- [25] U. Drescher and D. Brüggemann, Fluid selection for the organic Rankine cycle (ORC) in biomass power and heat plants, *Applied Thermal Engineering* 27 (2007) 223-228.
- [26] T. Yamamoto, T. Furuhashi, N. Arai, K. Mori, Design and testing of the organic Rankine cycle, *Energy* 26 (2001) 239-251.
- [27] R.L. Powell, CFC phase-out: Have we met the challenge? *Journal of Fluorine Chemistry* 114 (2002) 237-250.
- [28] H. Yamaguchi, X.R. Zhang, K. Fujima, M. Enomoto, N. Sawada, Solar energy powered Rankine cycle using supercritical CO₂, *Applied Thermal Engineering* 26 (2006) 2345-2354.
- [29] G. Angelino and P. Colonna di Paliano, Multicomponent working fluids for organic rankine cycles (ORCs), *Energy* 23 (1998) 449-463

[30] A. Borsukiewicz-Gozdur, W. Nowak, Comparative analysis of natural and synthetic refrigerants in application to low temperature Clausius-Rankine cycle, *Energy* 32 (2007) 344-352.

[31] V. Lemort, Testing and modeling scroll compressors with a view to integrate them as expanders into a Rankine cycle, DEA Thesis, University of Liege, 2006.

[32] Y.A. Cengel, M.A. Boles, *THERMODYNAMICS: An Engineering Approach*, 4th edition, McGraw-Hill, 2002.

[33] Meteonorm, (2005), *Global Meteorological Database for Engineers, Planers and Education*, Version 5.1.

[34] S.A. Klein, (2007), *Engineering Equation Solver (EES)*, Academic professional version.

List of figures

Fig. 1: Schematic of the low-temperature solar organic Rankine cycle with heat storage system

Fig. 2: T-s process diagram of the ORC

Fig. 3: Average Monthly Ambient Temperature for three locations: Bamako (Mali), Garoua (Cameroon) and Bangkok (Thailand).

Fig. 4: Turbine outlet volume flow rate versus turbine inlet temperature for various working fluids at $T_c = 35\text{ }^\circ\text{C}$.

Fig. 5: System thermal efficiency versus turbine inlet pressure for working fluids with low normal boiling points at $T_c = 35\text{ }^\circ\text{C}$ and $\Delta T_{ht} = 15\text{ }^\circ\text{C}$.

Fig. 6: System thermal efficiency versus turbine inlet pressure for working fluids with high normal boiling points at $T_c = 35\text{ }^\circ\text{C}$ and $\Delta T_{ht} = 15\text{ }^\circ\text{C}$.

Fig. 7: System second law efficiency versus turbine inlet pressure for working fluids with low normal boiling points at $T_c = 35\text{ }^\circ\text{C}$ and $\Delta T_{ht} = 15\text{ }^\circ\text{C}$.

Fig. 8: System second law efficiency versus turbine inlet pressure for working fluids with high normal boiling points at $T_c = 35\text{ }^\circ\text{C}$ and $\Delta T_{ht} = 15\text{ }^\circ\text{C}$.

Fig. 9: The distribution of irreversibility in different components for several fluids: R134a, R407C, RC318 and Ethanol.

Fig. 10: System total irreversibility rate versus turbine inlet pressure for working fluids with low normal boiling points at $T_c = 35\text{ }^\circ\text{C}$.

Fig. 11: System total irreversibility rate versus turbine inlet pressure for working fluids with high normal boiling points at $T_c = 35\text{ }^\circ\text{C}$.

Fig. 12: System total irreversibility rate versus turbine inlet pressure for working fluids with low normal boiling points at $T_c = 35\text{ }^\circ\text{C}$ and a heat source temperature of $90\text{ }^\circ\text{C}$.

Fig. 13: System total irreversibility rate versus turbine inlet pressure for working fluids with high normal boiling points at $T_c = 35\text{ }^\circ\text{C}$ and a heat source temperature of $90\text{ }^\circ\text{C}$.

Fig.14: Mass flow rate versus turbine inlet temperature for various working fluids at $T_c = 35\text{ }^\circ\text{C}$.

Fig. 15: Heat input rate versus turbine inlet temperature for various

working fluids at $T_c = 35 \text{ }^\circ\text{C}$.

Fig. 16: Components irreversibility versus ambient temperature
(R134a as working fluid)

Fig. 17: Second law efficiency and Total irreversibility versus ambient temperature
(R134a as working fluids)

Fig. 18: Diagram showing the heat exchange process between the hot water and
R134a in the upper heat exchangers.

Fig. 19: Diagram showing the heat exchange process between the hot water and
Methanol in the upper heat exchangers.

Fig. 20: Diagram showing the heat exchange process between the hot water and
R407C in the upper heat exchangers.

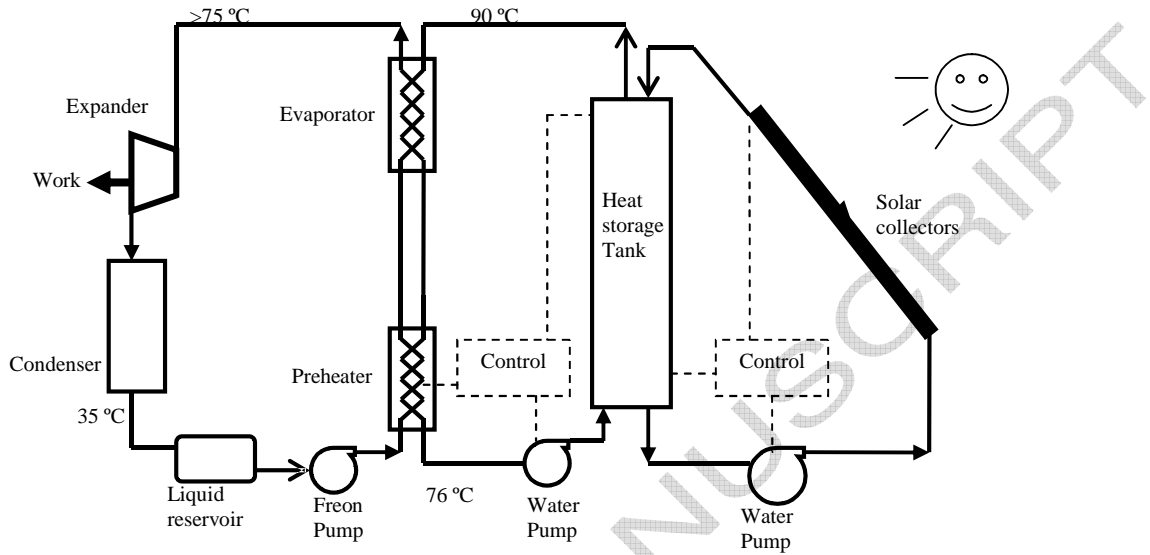


Fig. 1: Schematic of the low-temperature solar organic Rankine cycle with heat storage system

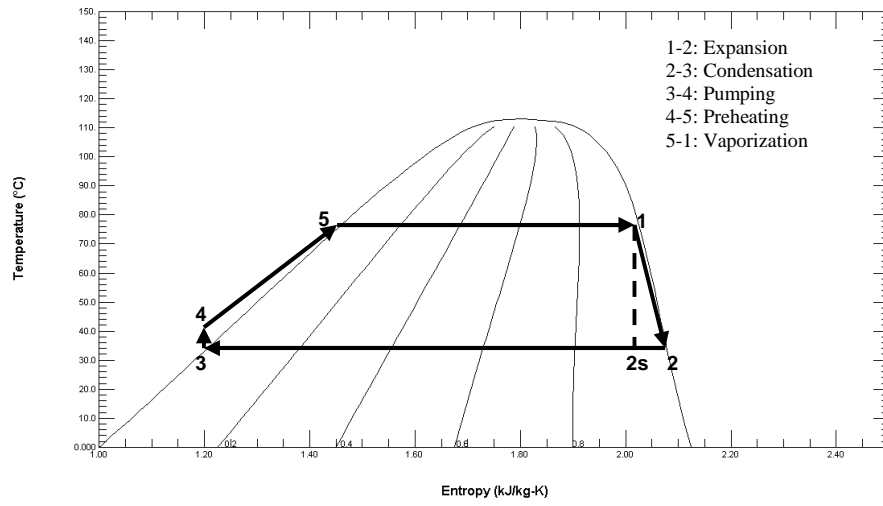


Fig. 2: T-s process diagram of the ORC

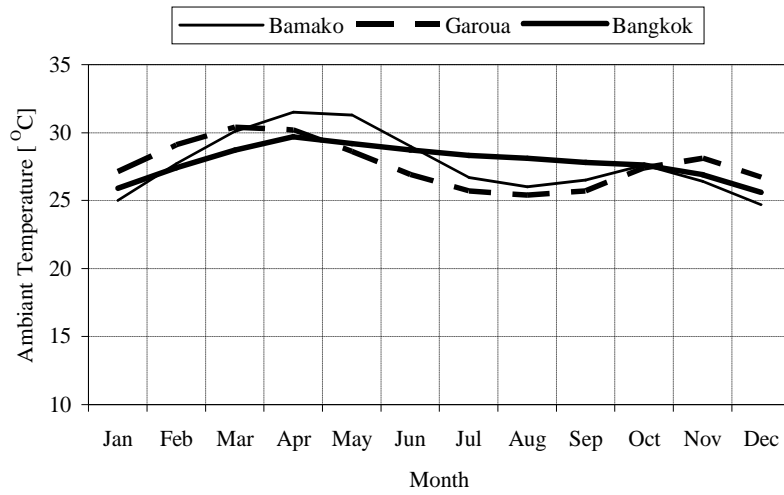


Fig. 3: Average Monthly Ambient Temperature for three locations: Bamako (Mali), Garoua (Cameroon) and Bangkok (Thailand).

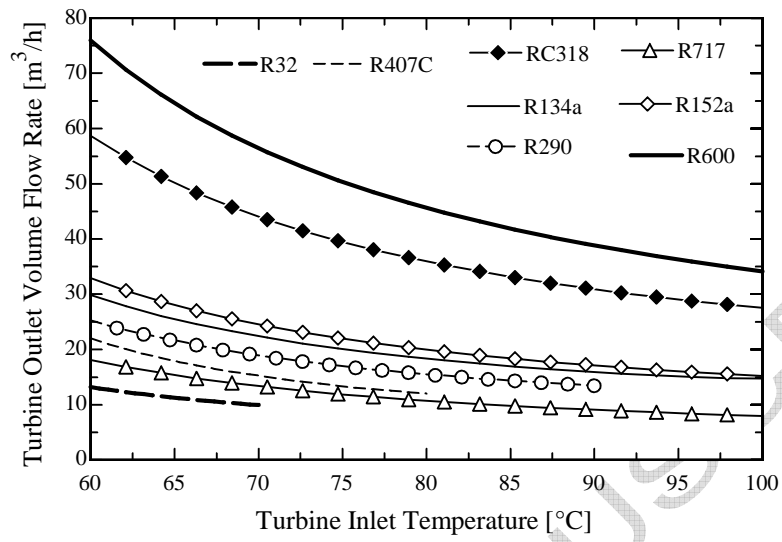


Fig. 4: Turbine outlet volume flow rate versus turbine inlet temperature for various working fluids at $T_c = 35\text{ }^\circ\text{C}$.

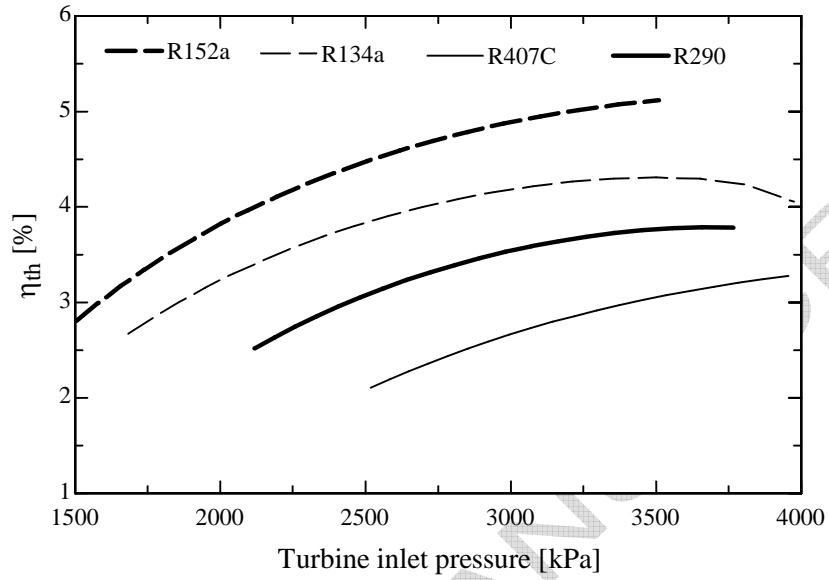


Fig. 5: System thermal efficiency versus turbine inlet pressure for working fluids with low normal boiling points at $T_c=35$ °C and $\Delta T_{ht}=15$ °C .

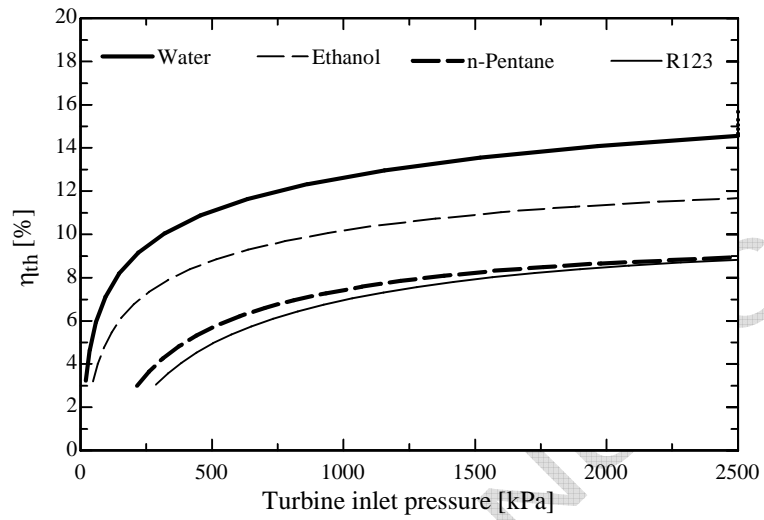


Fig. 6: System thermal efficiency versus turbine inlet pressure for working fluids with high normal boiling points at $T_c=35$ °C and $\Delta T_{ht}=15$ °C .

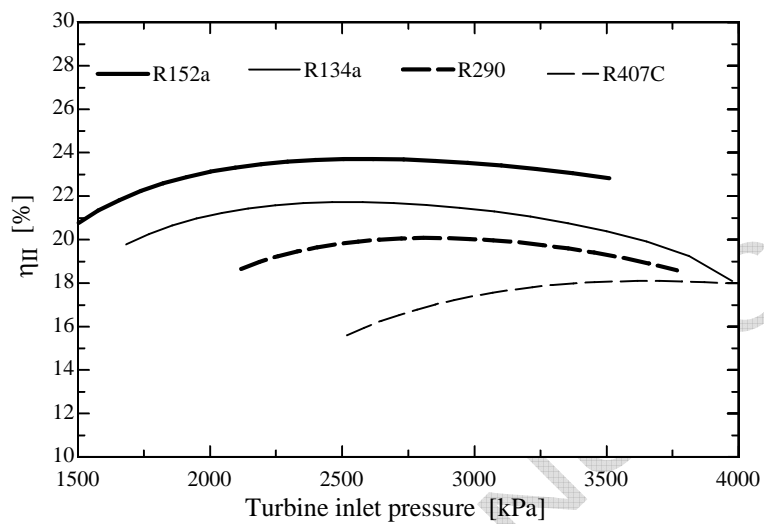


Fig. 7: System second law efficiency versus turbine inlet pressure for working fluids with low normal boiling points at $T_c=35$ °C and $\Delta T_{ht}=15$ °C .

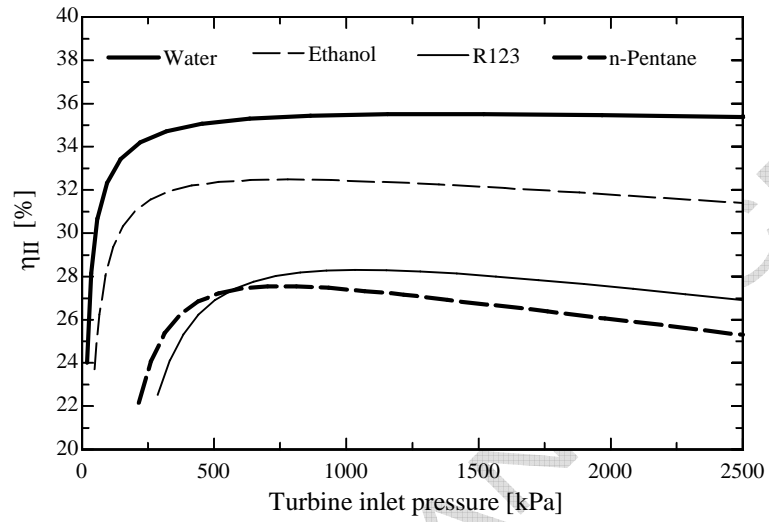


Fig. 8: System second law efficiency versus turbine inlet pressure for working fluids with high normal boiling points at $T_c = 35$ °C and $\Delta T_{ht} = 15$ °C.

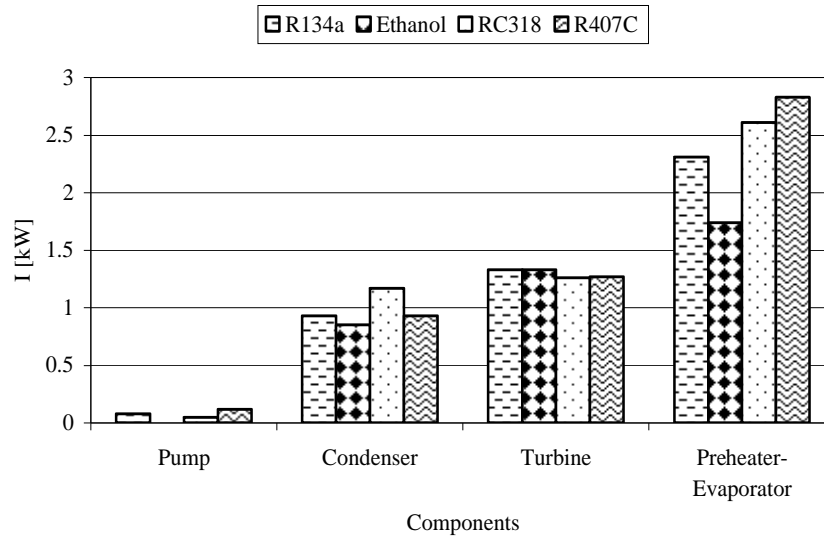


Fig. 9: The distribution of irreversibility in different components for several fluids: R134a, R407C, RC318 and Ethanol.

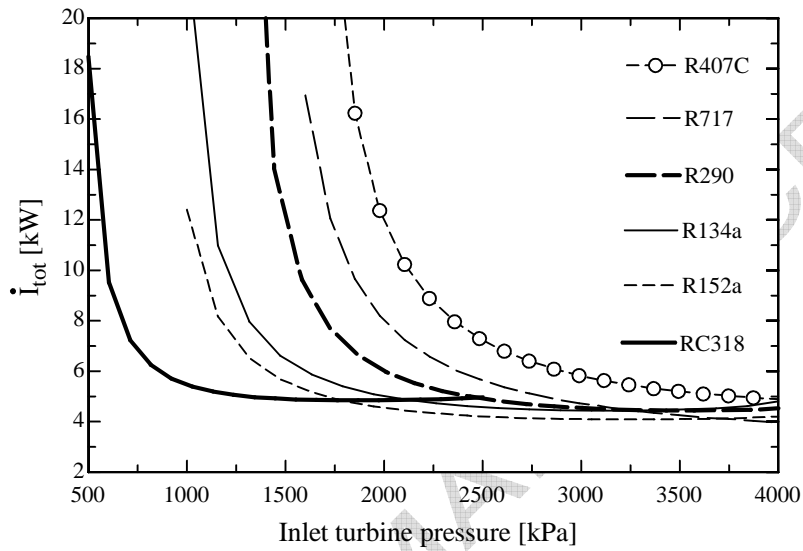


Fig. 10: System total irreversibility rate versus turbine inlet pressure for working fluids with low normal boiling points at $T_c=35$ °C.

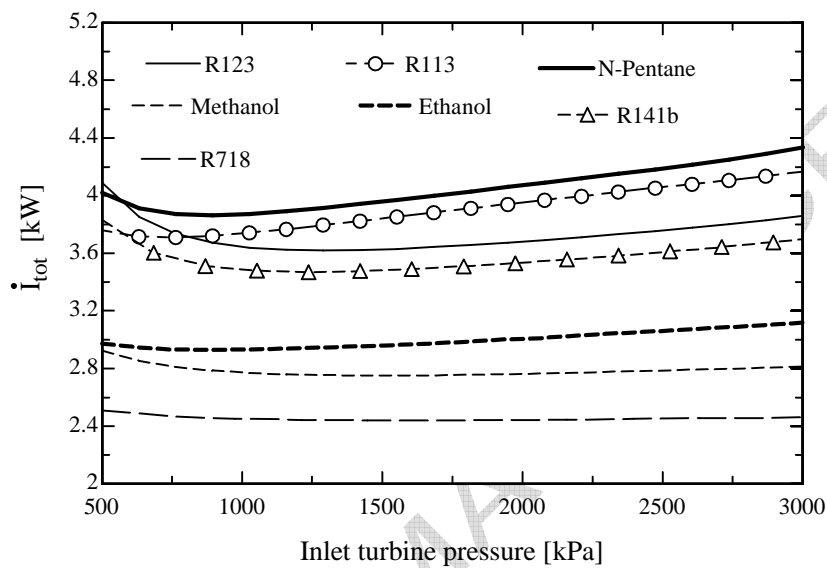


Fig. 11: System total irreversibility rate versus turbine inlet pressure for working fluids with high normal boiling points at $T_c=35$ °C.

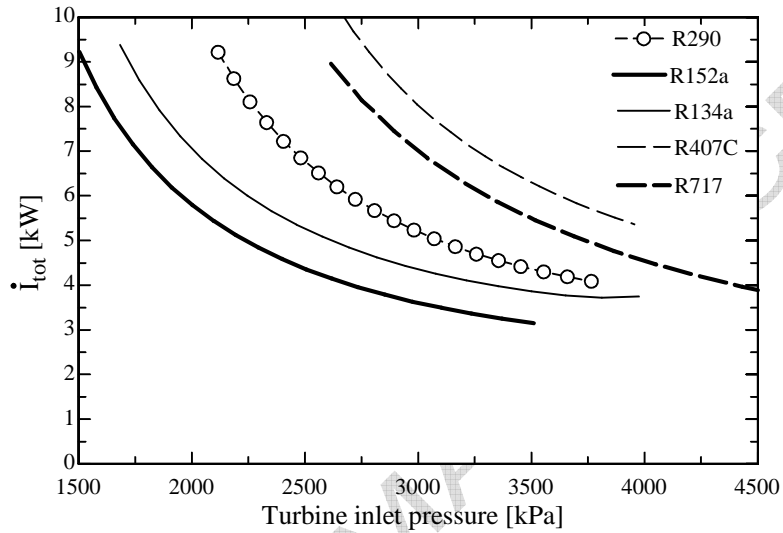


Fig. 12: System total irreversibility rate versus turbine inlet pressure for working fluids with low normal boiling points at $T_c=35$ °C and a heat source temperature of 90 °C.

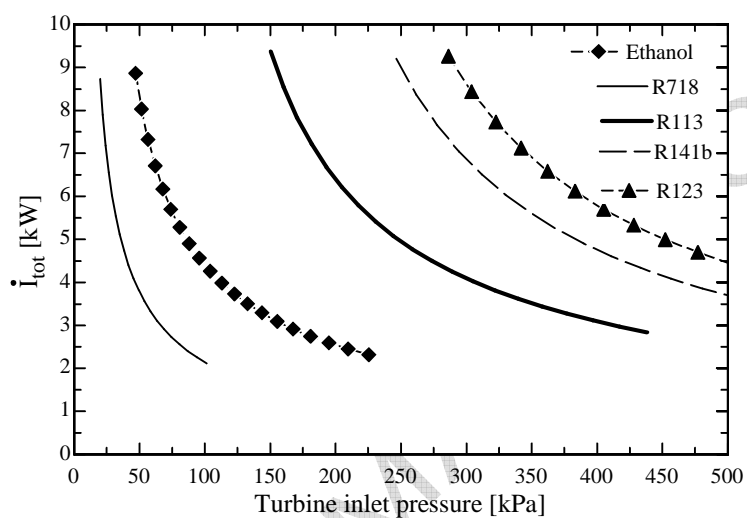


Fig. 13: System total irreversibility rate versus turbine inlet pressure for working fluids with high normal boiling points at $T_c=35$ °C and a heat source temperature of 90 °C.

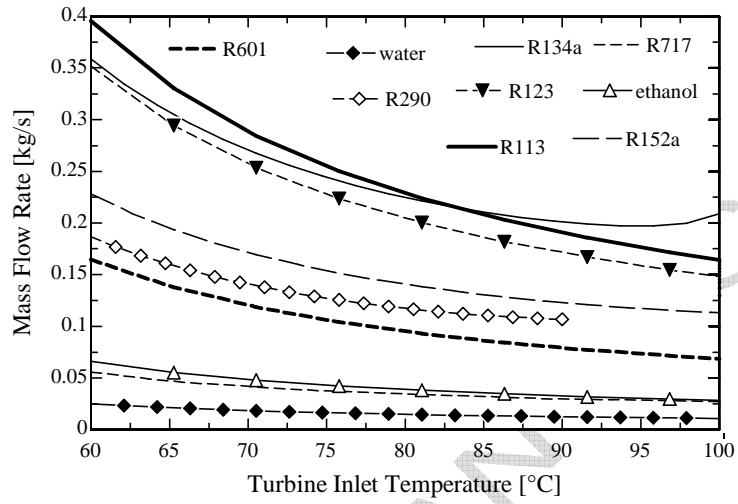


Fig. 14: Mass flow rate versus turbine inlet temperature for various working fluids at $T_c = 35 \text{ }^\circ\text{C}$.

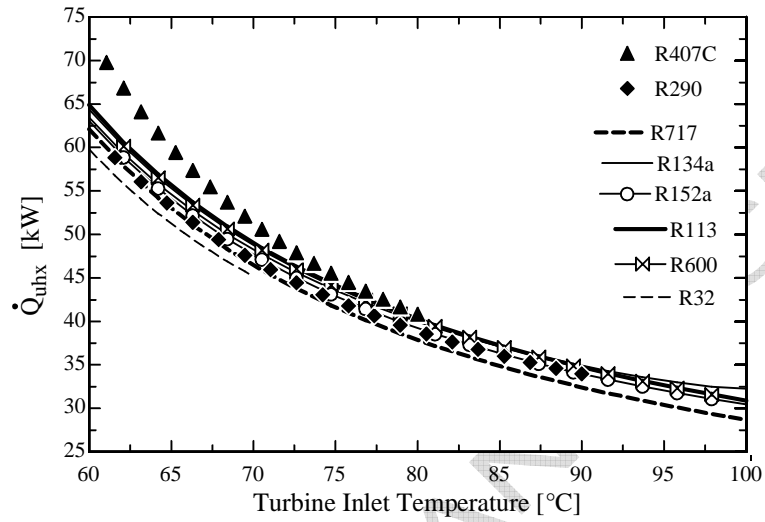


Fig. 15: Heat input rate versus turbine inlet temperature for various working fluids at $T_c = 35^{\circ}\text{C}$.

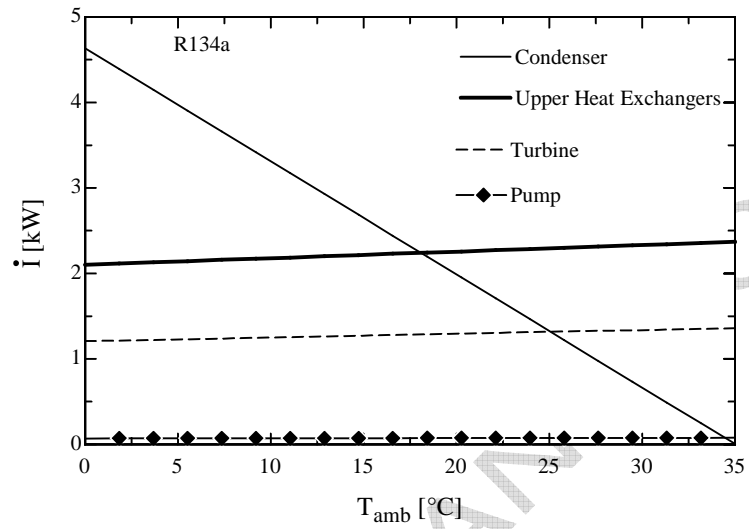


Fig. 16: Components irreversibility versus ambient temperature (R134a as working fluid)

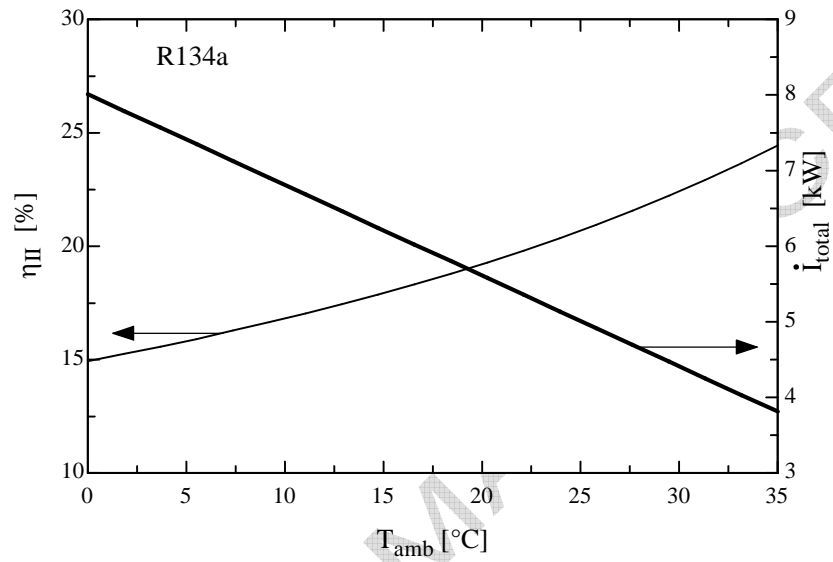


Fig. 17: Second law efficiency and Total irreversibility versus ambient temperature (R134a as working fluids)

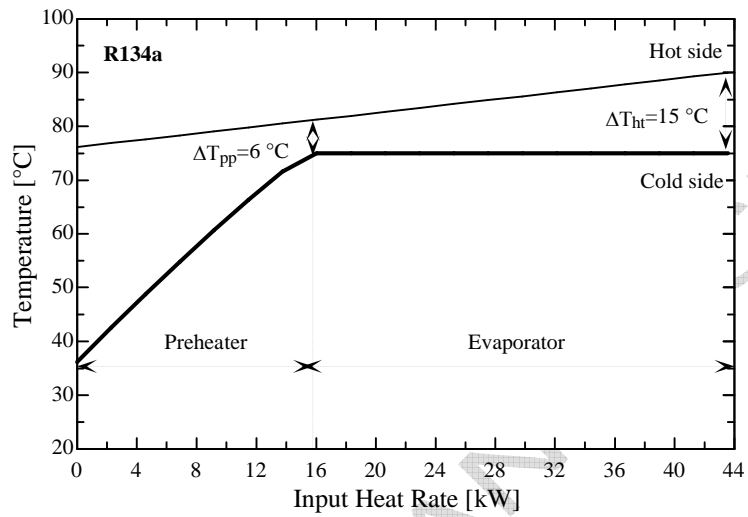


Fig. 18: Diagram showing the heat exchange process between the hot water and R134a in the upper heat exchangers.

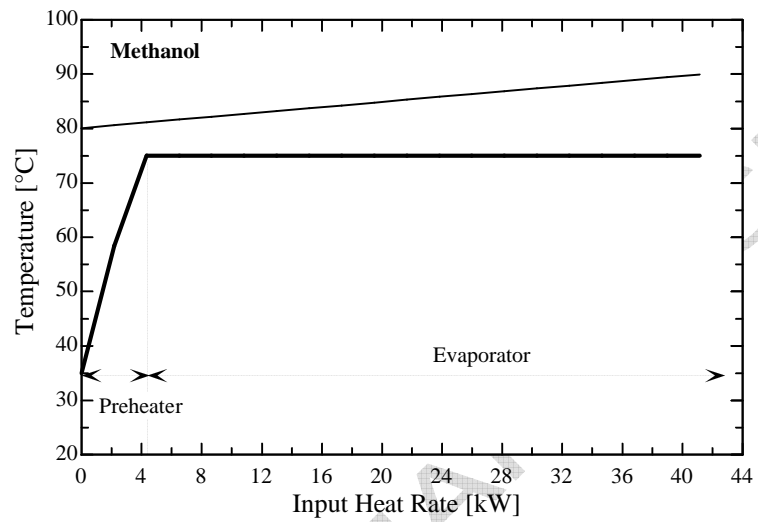


Fig. 19: Diagram showing the heat exchange process between the hot water and Methanol in the upper heat exchangers.

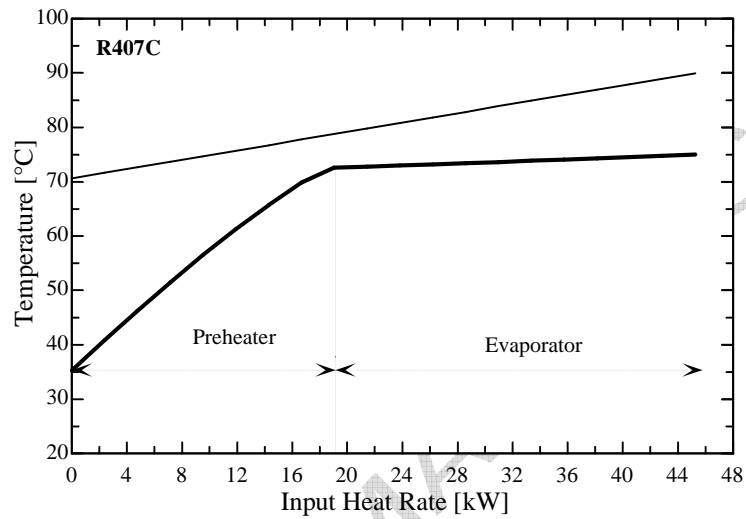


Fig. 20: Diagram showing the heat exchange process between the hot water and R407C in the upper heat exchangers.

List of tables

Table 1: Input data for the analysis of the ORC

Table 2: Physical, safety and environmental data of the working fluids

Table 3: Comparison of the performances of different working fluids for a 2 kW power output

*(i: isentropic; w: wet; d: dry), ^aR717: ammonia, ^bR718: water.

Table 4: Pinch analysis for the upper heat exchangers for five different working fluids (2kW power output, heat source temperature: 90 °C)

Table 5: Summary

Table 1: Input data for the analysis of the ORC

Evaporating temperature	T_e	75 °C
Condensing temperature	T_c	35 °C
Mechanical efficiency of the turbine	η_{mt}	0.63
Isentropic efficiency of the turbine	η_{st}	0.70
Pump efficiency	η_p	0.80

Table 2: Physical, safety and environmental data of the working fluids

Substance	Physical data			Safety data	Environmental data				
	Molecular Mass (kg/kmol)	^a T_{bp} (°C)	^b T_{crit} (°C)	^c P_{crit} (MPa)	ASHRAE 34 safety group	Atmospheric life time (yr)	^d ODP	^e GWP (100 yr)	
1	RC318	200.03	-6.0	115.2	2.778	A1	3200	0	10250
2	R600a	58.12	-11.7	135	3.647	A3	0.019	0	~20
3	R114	170.92	3.6	145.7	3.289	A1	300	1.000	10040
4	R600	58.12	-0.5	152	3.796	A3	0.018	0	~20
5	R601	72.15	36.1	196.5	3.364	-	0.01	0	~20
6	R113	187.38	47.6	214.1	3.439	A1	85	1.000	6130
7	Cyclohexane	84.16	80.7	280.5	4.075	A3	n.a	n.a	n.a
8	R290	44.10	-42.1	96.68	4.247	A3	0.041	0	~20
9	R407C	86.20	-43.6	86.79	4.597	A1	n.a	0	1800
10	R32	52.02	-51.7	78.11	5.784	A2	4.9	0	675
11	R500	99.30	-33.6	105.5	4.455	A1	n.a	0.738	8100
12	R152a	66.05	-24.0	113.3	4.520	A2	1.4	0	124
13	R717 (Ammonia)	17.03	-33.3	132.3	11.333	B2	0.01	0	<1
14	Ethanol	46.07	78.4	240.8	6.148	n.a	n.a	n.a	n.a
15	Methanol	32.04	64.4	240.2	8.104	n.a	n.a	n.a	n.a
16	R718 (Water)	10.2	100	374	22.064	A1	n.a	0	<1
17	R134a	102.03	-26.1	101	4.059	A1	14.0	0	1430
18	R12	120.91	-29.8	112	4.114	A1	100	1.000	10890
19	R123	152.93	27.8	183.7	3.668	B1	1.3	0.020	77
20	R141b	116.95	32.0	204.2	4.249	n.a	9.3	0.120	725

^a T_{bp} : Normal boiling point; ^b T_{crit} : Critical temperature; ^c P_{crit} : Critical pressure;

^dODP: ozone depletion potential, relative to R-11; ^eGWP: Global warming potential, relative to CO₂.

n.a: non available

Table 3: Comparison of the performances of different working fluids for a 2 kW power output

*(i: isentropic; w: wet; d: dry), ^aR717: ammonia, ^bR718: water.

Substance	Type*	P_{\min} [MPa]	P_{\max} [MPa]	PR	\dot{V}_2 [m ³ /h]	VFR (\dot{V}_2/\dot{V}_1)	v_2 (m ³ /kg)	\dot{m}_{wf} [kg/s]	η_{th} [%]	η_{II} [%]	φ [%]	\dot{I}_{tot} [kW]	\dot{Q}_{uhx} [kW]	Δh_{fg} [kJ/kg]	x_2	
1	RC318	d	0.425	1.201	2.825	39.48	3.294	0.028	0.381	3.715	21.76	61.48	5.104	47.01	75.83	1
2	R600a	d	0.463	1.191	2.57	39.02	2.802	0.088	0.122	4.055	23.75	71.07	4.579	44.20	255.7	1
3	R114	d	0.290	0.826	2.84	55.57	3.025	0.050	0.305	4.122	24.14	70.96	4.659	45.04	104.6	1
4	R600	d	0.329	0.907	2.758	50.36	2.893	0.128	0.108	4.236	24.81	74.21	4.462	43.91	300.2	1
5	R601	d	0.098	0.323	3.285	141	3.307	0.369	0.106	4.367	25.58	76.65	4.501	44.67	323	1
6	R113	d	0.065	0.232	3.558	197.7	3.52	0.215	0.254	4.456	26.1	77.85	4.391	44.11	134.8	1
7	Cyclohexane	d	0.020	0.084	4.232	557.7	4.038	1.58	0.098	4.609	27	81.8	4.206	43.17	360	1
8	R290	w	1.218	2.85	2.34	16.99	2.717	0.037	0.127	3.428	20.08	63.1	4.614	42.43	210.4	0.987
9	R407C	w	1.535	3.735	2.433	13.34	2.611	0.014	0.250	3.087	18.08	59.3	5.155	45.26	102.9	0.913
10	R32	w	2.19	5.417	2.474	9.019	3.015	0.011	0.212	2.611	15.3	46.51	4.724	40.79	89.28	0.728
11	R500	w	1.001	2.475	2.473	18.98	2.72	0.020	0.256	3.712	21.74	68.13	4.508	42.53	113.1	0.987
12	R152a	w	0.794	2.108	2.652	21.95	2.839	0.039	0.154	3.985	23.34	71.81	4.443	42.92	200.2	0.977
13	^a R717	w	1.351	3.709	2.746	11.87	2.627	0.087	0.037	4.352	25.49	81.85	4.121	41.63	907.5	0.917
14	Ethanol	w	0.013	0.088	6.468	610.6	5.841	3.951	0.042	4.796	28.09	88.2	3.932	41.59	854.6	0.982
15	Methanol	w	0.027	0.148	5.416	336.1	4.725	2.704	0.034	4.845	28.38	90.77	3.856	41.14	1082	0.952
16	^b R718	w	0.005	0.038	6.854	1413	5.784	23.93	0.016	4.899	28.7	93.28	3.793	40.81	2321	0.949
17	R134a	i	0.887	2.366	2.666	20.1	3.056	0.022	0.244	3.703	21.69	64.94	4.651	43.57	115.8	0.992
18	R12	i	0.847	2.086	2.463	22.43	2.679	0.020	0.301	3.835	22.46	70.06	4.465	42.60	99.15	1
19	R123	i	0.130	0.431	3.298	104.9	3.304	0.128	0.227	4.457	26.11	77.48	4.318	43.54	148.2	1
20	R141b	i	0.112	0.371	3.309	121.7	3.234	0.195	0.173	4.526	26.51	80.21	4.242	43.17	199.7	1

Table 4: Pinch analysis for the upper heat exchangers for five different working fluids
(2kW power output, heat source temperature: 90 °C)

Substance	$T_{0,hf}$ [°C]	$T_{pp,hf}$ [°C]	$T_{pp,wf}$ [°C]	\dot{m}_{wf} (kg/s)	\dot{m}_{hft} (kg/s)	\dot{Q}_{uhx} (kW)
R134a	76.14	81	75	0.244	0.75	43.57
R407C	70.61	78.5	72.5	0.260	0.56	45.26
R152a	77.47	81	75	0.154	0.82	42.92
Ammonia	79	81	75	0.037	0.90	41.63
Methanol	80.10	81	75	0.034	0.99	41.14

Table 5: Summary

Substances		Calculated data								Safety data		Environmental data		Decision
Names	P_{\min}	P_{\max}	PR	\dot{V}_2	η_{th}	η_{II}	\dot{I}_{tot}	φ_e	x_2	Toxicity	Flammability	ODP	GWP	A/R
1	RC318	+	+	+	+	+	+	-	-	+	+	+	-	+/-
2	R600a	+	+	+	+	+	+	+	+	+	-	+	+	accepted
3	R114	+	+	+	+	+	-	+	+	+	+	-	-	<i>rejected</i>
4	R600	+	+	+	+	+	+	+	+	+	-	+	+	accepted
5	R601	+	+	+	-	+	+	+	+	+	-	+	+	<i>rejected</i>
6	R113	-	+	+	-	+	+	+	+	+	+	-	-	<i>rejected</i>
7	Cyclohexane	-	-	-	-	+	+	+	+	+	-	n.a	n.a	<i>rejected</i>
8	R290	+	+	+	+	-	-	-	-	+	-	+	+	accepted
9	R407C	+	-	+	+	-	-	-	+/-	+	+	+	+	+/-
10	R32	+	-	+	+	-	-	-	-	+	+/-	+	+	<i>rejected</i>
11	R500	+	+	+	+	+	+	+	+	+	+	-	-	<i>rejected</i>
12	R152a	+	+	+	+	+	+	+	+	+	+/-	+	+	accepted
13	Ammonia	+	-	+	+	+	+	+	+	+/-	-	+	+	+/-
14	Ethanol	-	-	-	-	+	+	+	+	+	-	n.a	n.a	<i>rejected</i>
15	Methanol	-	+	-	-	+	+	+	+	-	-	n.a	n.a	<i>rejected</i>
16	Water	-	-	-	-	+	+	+	+	+	+	+	+	<i>rejected</i>
17	R134a	+	+	+	+	+	-	+	+	+	+	+	+	accepted
18	R12	+	+	+	+	+	+	+	+	+	+	-	-	<i>rejected</i>
19	R123	+	+	+	-	+	+	+	+	-	+	-	+	<i>rejected</i>
20	R141b	+	+	+	-	+	+	+	+	+	n.a	-	+	<i>rejected</i>